

Synthesis and Two-Photon Absorption Properties of 9,10-Bis(arylethynyl)anthracene Derivatives

Wen Jun Yang, Chang Ho Kim, Mi-Yun Jeong, Seung Kyu Lee, Ming Jun Piao, Seung-Joon Jeon,* and Bong Rae Cho*

Molecular Opto-Electronics Laboratory, Department of Chemistry and Center for Electro- and Photo-Responsive Molecules, Korea University, 1-Anamdong, Seoul, 136-701 Korea

Received October 18, 2003. Revised Manuscript Received April 30, 2004

A series of 9,10-bis(arylethynyl)anthracene derivatives (**1–8**) have been synthesized and their two-photon absorption (TPA) cross sections were measured by nanosecond fluorescence measurement and femtosecond Z-scan methods. The λ_{max} values of these molecules are very similar and the $\lambda_{\text{max}}^{(2)}$ values are near 800 nm. The $\delta_{\text{max}}^{\text{ns}}/\text{MW}$ of the dipole increases with the conjugation length, whereas those for the quadrupoles decrease slightly with MW. Also, the $\delta_{\text{max}}^{\text{ns}}/\text{MW}$ of the octupole is smaller than the dipole. In all cases, $\delta_{\text{max}}^{\text{ns}}/\text{MW}$ of the quadrupoles are larger than the dipoles. Moreover, the results of the femtosecond Z-scan experiment indicate significant contribution by the excited-state absorption in $\delta_{\text{max}}^{\text{ns}}$. Noteworthy is the good agreement between the structure–TPA property relationships determined by both methods.

Introduction

There is contemporary research effort to synthesize organic materials exhibiting large two-photon absorption (TPA) cross sections (δ_{TPA}) for possible applications in a number of new areas including three-dimensional fluorescence imaging, optical limiting, photodynamic therapy, and three-dimensional optical data storage and microfabrication.^{1–14} Among the most extensively investigated compounds are donor-bridge-acceptor (D- π -A) dipoles, donor-bridge-donor (D- π -D) quadrupoles, multi-branched compounds, dendrimers, and octupoles.^{15–22} The results of structure–property relationship studies reveal that the δ_{TPA} increases with the donor/acceptor strength, chain length, and planarity of the

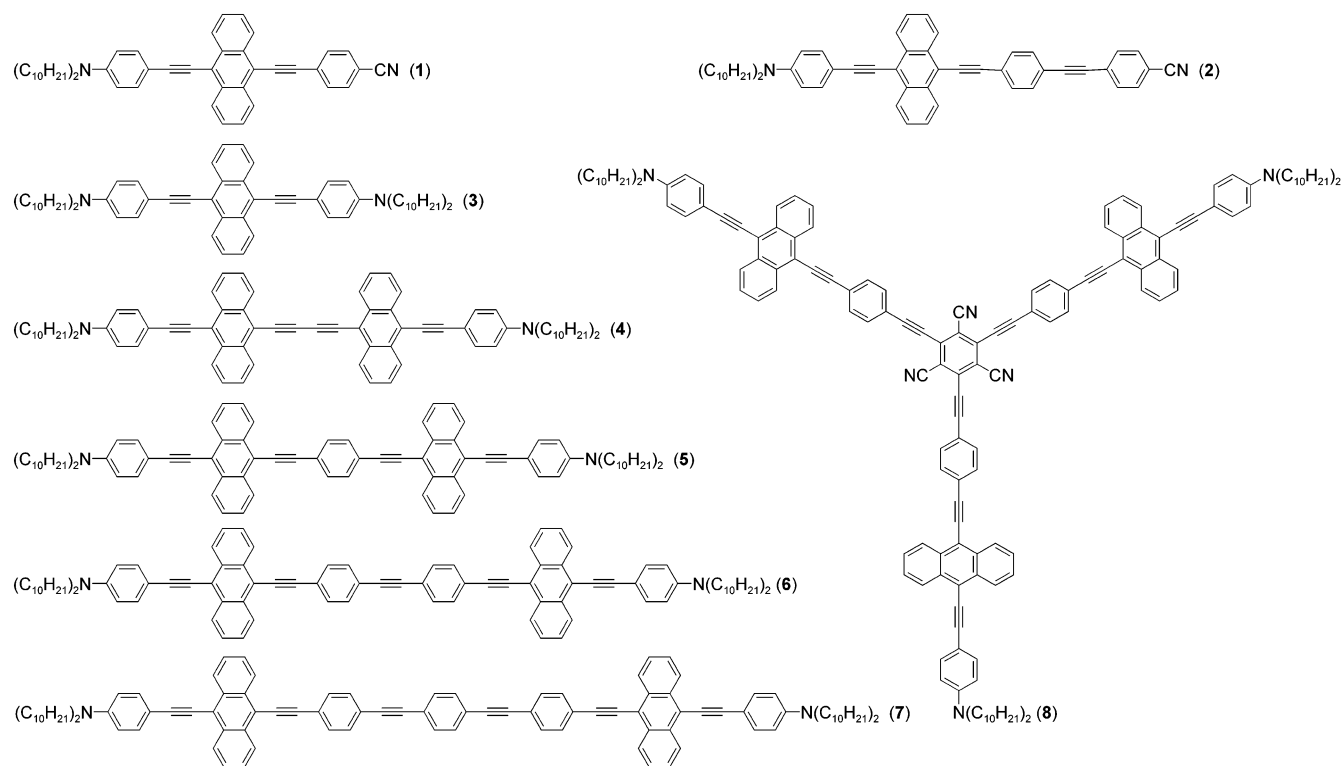
π -center. Most of these studies employed C=C bonds as the conjugation bridge and phenyl, biphenyl, fluo-

* To whom correspondence should be addressed. Tel.: 82-2-3290-3129. E-mail: chobrr@korea.ac.kr. Fax: 82-2-3290-3121.

- (1) Denk, W.; Stricker, J. H.; Webb, W. W. *Science* **1990**, *248*, 73.
- (2) Spangler, C. W. *J. Mater. Chem.* **1999**, *9*, 2013.
- (3) Maruo, S.; Nakamura, O.; Kawata, S. *Opt. Lett.* **1997**, *22*, 132.
- (4) Zhou, W.; Kuebler, S. M.; Braum, K. L.; Yu, T.; Cammack, J. K.; Ober, C. K.; Perry, J. W.; Marder, S. R. *Science* **2002**, *296*, 1106.
- (5) Tutt, L. W.; Boggess, T. F. *Prog. Quantum Electron* **1993**, *17*, 299.
- (6) He, G. S.; Xu, G. C.; Prasad, P. N.; Reinhardt, B. A.; Bhatt, J. C.; Dillard, A. G. *Opt. Lett.* **1995**, *20*, 435.
- (7) He, G. S.; Weder, C.; Smith, P.; Prasad, P. N. *IEEE J. Quantum Electron* **1998**, *34*, 2279.
- (8) Hell, S. W.; Hanninen, P. E.; Kuusisto, A.; Schrader, M.; Soini, E. *Opt. Commun.* **1995**, *117*, 20.
- (9) Bhawalkar, J. D.; Kumar, N. D.; Swiatkiewicz, J.; Prasad, P. N. *Nonlinear Opt.* **1998**, *19*, 249.
- (10) Joshi, M. P.; Pudavar, H. E.; Swiatkiewicz, J.; Prasad, P. N.; Reinhardt, B. A. *Appl. Phys. Lett.* **1999**, *74*, 170.
- (11) He, G. S.; Swiatkiewicz, J.; Jiang, Y.; Prasad, P. N.; Reinhardt, B. A.; Tan, L.-S.; Kannan, R. *J. Phys. Chem. A* **2000**, *104*, 4805.
- (12) Bhawalkar, J. D.; Kumar, N. D.; Zhao, C. F.; Prasad, P. N. *J. Clin. Laser Med. Surg.* **1997**, *15*, 201.
- (13) Cumpston, B. H.; Ananthavel, S. P.; Barlow, S.; Dyer, D. L.; Ehrlich, J. E.; Erskine, L. L.; Heikal, A. A.; Kuebler, S. M.; Lee, I.-Y. S.; McCord-Maughon, D.; Qin, J.; Röckel, H.; Rumi, M.; Wu, X.-L.; Marder, S. R.; Perry, J. W. *Nature* **1999**, *398*, 51.
- (14) Kawata, S.; Sun, H.-B.; Tanaka, T.; Takata, K. *Nature* **2001**, *412*, 697.

- (15) (a) Reinhardt, B. A.; Brott, L. L.; Clarson, S. J.; Dillard, A. G.; Bhatt, J. C.; Kannan, R.; Yuan, L.; He, G. S.; Prasad, P. N. *Chem. Mater.* **1998**, *10*, 1863. (b) Belfield, K. D.; Hagan, D. J.; Van Stryland, E. W.; Schafer, K. J.; Negres, R. A. *Org. Lett.* **1999**, *1*, 1575. (c) Belfield, K. D.; Schafer, K. J.; Mourad, W.; Reinhardt, B. A. *Org. Chem.* **2000**, *65*, 4475. (d) Abbotto, A.; Beverina, L.; Bozio, R.; Facchetti, A.; Ferrante, C.; Pagani, G. A.; Pedron, D.; Signorini, R. *Org. Lett.* **2002**, *4*, 1495.
- (16) Kim, O.-K.; Lee, K.-S.; Woo, H. Y.; Kim, K.-S.; He, G. S.; Swiatkiewicz, J.; Prasad, P. N. *Chem. Mater.* **2000**, *12*, 284.
- (17) (a) Albota, M.; Beljonne, D.; Brédas, J.-L.; Ehrlich, J. E.; Fu, J.-Y.; Heikal, A. A.; Hess, S. E.; Kogej, T.; Levin, M. D.; Marder, S. R.; McCord-Maughon, D.; Perry, J. W.; Röckel, H.; Rumi, M.; Subramaniam, G.; Webb, W. W.; Wu, X.-L.; Xu, C. *Science* **1998**, *281*, 1653. (b) Rumi, M.; Ehrlich, J. E.; Heikal, A. A.; Perry, J. W.; Barlow, S.; Hu, Z.; McCord-Maughon, D.; Parker, T. C.; Röckel, H.; Thayumanavan, S.; Marder, S. R.; Beljonne, D.; Brédas, J.-L. *J. Am. Chem. Soc.* **2000**, *122*, 9500. (c) Pond, S. J. K.; Rumi, M.; Levin, M. D.; Parker, T. C.; Beljonne, D.; Day, M. W.; Brédas, J.-L.; Marder, S. R.; Perry, J. W. *J. Phys. Chem. A* **2002**, *106*, 11470.
- (18) (a) Ventelon, L.; Charier, S.; Moreaux, L.; Mertz, J.; Blanchard-Desce, B. *Angew. Chem., Int. Ed.* **2001**, *40*, 2098. (b) Mongin, O.; Porres, L.; Moreaux, L.; Mertz, J.; Blanchard-Desce, M. *Org. Lett.* **2002**, *4*, 719. (c) Ogawa, K.; Ohashi, A.; Kobuke, Y.; Kamada, K.; Ohta, K. *J. Am. Chem. Soc.* **2003**, *125*, 13356. (d) Iwase, Y.; Kamada, K.; Ohta, K.; Kondo, K. *J. Mater. Chem.* **2003**, *13*, 1575.
- (19) (a) Chung, S.-J.; Kim, K.-S.; Lin, T.-C.; He, G. S.; Swiatkiewicz, J.; Prasad, P. N. *J. Phys. Chem. B* **1999**, *103*, 10741. (b) Macak, P.; Luo, Y.; Norman, H.; Agren, H. *J. Chem. Phys.* **2000**, *113*, 7055.
- (20) Adronov, A.; Fréchet, J. M.; He, G. S.; Kim, K.-S.; Chung, S.-J.; Swiatkiewicz, J.; Prasad, P. N. *Chem. Mater.* **2000**, *12*, 2838.
- (21) (a) Lee, W.-H.; Cho, M.; Jeon, S.-J.; Cho, B. R. *J. Phys. Chem. A* **2004**, *104*, 11033. (b) Cho, B. R.; Son, K. H.; Lee, S. H.; Song, Y.-S.; Lee, Y.-K.; Jeon, S.-J.; Choi, J.-H.; Lee, H.; Cho, M. *J. Am. Chem. Soc.* **2001**, *123*, 10039. (c) Lee, W.-H.; Lee, H.; Kim, J.-A.; Choi, J.-H.; Cho, M.; Jeon, S.-J.; Cho, B. R. *J. Am. Chem. Soc.* **2001**, *123*, 10658. (d) Cho, B. R.; Piao, M. J.; Son, K. H.; Lee, S. H.; Yoon, S. J.; Jeon, S.-J.; Choi, J.-H.; Lee, H.; Cho, M. *Chem. Eur. J.* **2002**, *8*, 3907. (e) Yoo, J.; Yang, S. K.; Jeong, M.-Y.; Ahn, H. C.; Jeon, S.-J.; Cho, B. R. *Org. Lett.* **2003**, *5*, 645.
- (22) (a) Ventelon, L.; Moreaux, L.; Mertz, J.; Blanchard-Desce, M. *Chem. Commun.* **1999**, 2055. (b) Zojer, E.; Beljonne, D.; Kogej, T.; Vogel, H.; Marder, S. R.; Perry, J. W.; Bredas, J. L. *J. Chem. Phys.* **2002**, *116*, 3646. (c) Beljonne, D.; Wenseleers, W.; Zojer, E.; Shuai, Z.; Vogel, H.; Pond, S. J. K.; Perry, J. W.; Marder, S. R.; Bredas, J. L. *Adv. Funct. Mater.* **2002**, *12*, 631. (d) Drobizhev, M.; Karotki, A.; Rebane, A.; Spangler, C. W. *Opt. Lett.* **2001**, *26*, 1081.

Chart 1



rene, dithieniothiophene, and dihydrophenanthrene as the π -centers, respectively.

It is well-established that δ_{TPA} increases with the extent of the charge transfer.^{21a-c} Although the C=C bond is an excellent conjugation bridge for the internal charge transfer (ICT) from the donor to the acceptor, it readily undergoes trans to cis photoisomerization. Because the TPA materials are photoexcited by the two-photon process, such possibility always exists and may hamper the efficiency and the lifetime of the materials. This problem could be avoided if one uses triple bonds as the conjugation bridge. However, little is known about the TPA materials containing the triple bond (C \equiv C). Moreover, anthracene might be a useful π -center not only because it is an excellent fluorophore but also because its derivatives have been extensively used as the fluorescence sensors.²³ Hence, if such derivatives with large δ_{TPA} are synthesized, it might be possible to develop two-photon sensors for biological applications. Very recently, we reported that 2,6-bis(styryl)anthracene derivatives show large TPA cross sections, which may be useful for such purpose.²⁴ In this work, we have synthesized 9,10-bis(arylethynyl)anthracene derivatives (**1–8**) as a new series of anthracene-based TPA chromophores and measured their TPA cross sections by both two-photon-induced fluorescence measurement and femtosecond Z-scan methods (Chart 1). Because most of the studies on the TPA chromophores are based on either of these methods, this result would provide a better insight into the structure–TPA property relationship.

We were interested in learning (i) the effectiveness of the C=C bond as the conjugation bridge, (ii) the influence of dipolar (**1,2**), quadrupolar (**3–7**), and octupolar (**8**) symmetry and the conjugation length on the δ_{TPA} , (iii) the contribution of the excited-state absorption to the TPA cross section measured by the nanosecond pulses ($\delta_{\text{max}}^{\text{ns}}$), and (iv) the structure–TPA property relationships determined by both methods. The results of these studies are reported here.

Results and Discussion

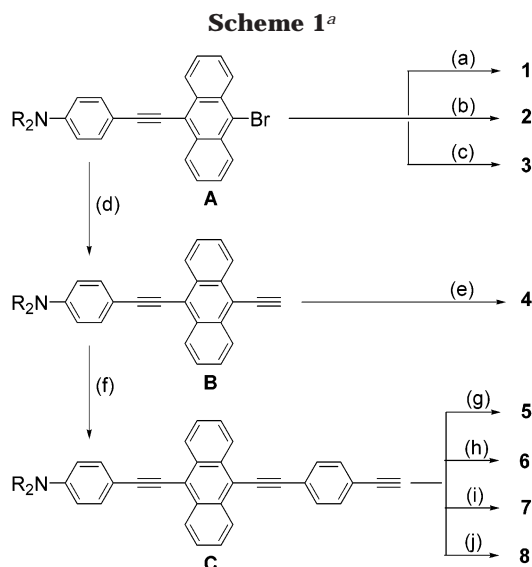
Synthesis. 9,10-Bis(arylethynyl)anthracene derivatives have been synthesized by Sonogashira coupling as shown in Scheme 1.²⁵ **A** was prepared by the coupling between *p*-didecylaminophenylacetylene and 9,10-dibromoanthracene in reasonable yield. Reaction of **A** with TMSacetylene followed by deprotection produced **B** in high yield. **C** was prepared by the reaction between **B** and diiodobenzene, followed by the coupling with TMSacetylene and deprotection. Compounds **1–3** were synthesized from **A** and appropriate arylacetylenes in modest to high yields. **4** was obtained by the homo coupling of **B**, and **5–8** were prepared by the reaction between **C** and appropriate aryl bromides, respectively, in modest to high yields. The structures of **1–8** were unambiguously confirmed by IR, ¹H, and ¹³C NMR and elemental analysis.

One-Photon Absorbance and Emission Spectra. Table 1 shows that the λ_{max} of **1** is 497 nm, which is red-shifted by more than 110 nm from the closely related 4-[4-(4-diethylaminophenylethynyl)phenylethynyl]benzonitrile ($\lambda_{\text{max}} = 382$ nm). Because the anthracenyl group has smaller aromatic resonance energy than

(23) (a) Mason, W. T. *Fluorescent and Luminescent Probes for Biological Activity*, 2nd ed.; Academic Press: New York, 1999. (b) de Silva, A. P.; Gunaratne, H. Q. N.; Gunlaugsson, T.; Huxley, A. J. M.; McCoy, C. P.; Rademacher, J. T.; Rice, T. E. *Chem. Rev.* **1997**, *97*, 1515.

(24) Yang, W. J.; Kim, D. Y.; Jeong, M.-Y.; Kim, H. M.; Jeon, S.-J.; Cho, B. R. *Chem. Commun.* **2003**, 2618.

(25) Takahashi, S.; Kuroyara, Y.; Sonogashira, K.; Hagihara, N. *Synthesis* **1980**, *8*, 627.



Reagents and conditions: (a) $p\text{-CNC}_6\text{H}_4\text{C}\equiv\text{CH}/\text{cat(I)}$, 60 °C, 32%; (b) $p\text{-CNC}_6\text{H}_4\text{C}\equiv\text{CC}_6\text{H}_4\text{C}\equiv\text{CH}/\text{cat(I)}$, 60 °C, 36%; (c) $p\text{-(C}_{10}\text{H}_{21})_2\text{NC}_6\text{H}_4\text{C}\equiv\text{CH}/\text{cat(II)}$, 85 °C, 75%; (d) TMS-acetylene/ cat(I) , 0 °C–RT, MeOH/THF/KOH(aq), RT, 87%; (e) **B**/ cat(I) , 60 °C, 69%; (f) (i) 1,4-diiodobenzene/ cat(I) , 50 °C, 68%, (ii) (d); (g) **A**/ cat(I) , 60 °C, 57%; (h) (i) (f)(i), (ii) **C**/ cat(I) , 60 °C, 63%; (i) (f)(i); 1,4-diiodobenzene/ cat(I) , 60 °C, 71%; (j) **C**/1,3,5-tribromo-2,4,6-tricyanobenzene/ cat(III) , 85 °C, 30%. $\text{cat(I)} = \text{Pd(PPh}_3)_2\text{Cl}_2/\text{CuI}/\text{Et}_3\text{N/THF}$, $\text{cat(II)} = \text{Pd(PPh}_3)_2\text{Cl}_2/\text{CuI}/\text{Et}_3\text{N/toluene}$, $\text{cat(III)} = \text{Pd(PPh}_3)_4/\text{CuI}/\text{Et}_3\text{N/toluene}$.

Table 1. One- and Two-Photon Properties of 9,10-Bis(arylethynyl)anthracene Derivatives (1–8)

cmpd	λ_{max}^a ($10^4 \epsilon^b$)	λ_{fl}^c	$\Delta\nu_{\text{ST}}^d$	Φ^e	$\lambda_{\text{max}}^{(2)f}$	$\delta_{\text{max}}^{\text{ns}g}$	$\delta_{\text{max}}^{\text{ns}}/\text{MW}^h$
1	497 (4.01)	556	2135	0.46	780 (990)	210 (250)	0.47 (0.56)
2	492 (4.39)	553	2242	0.45	780 (990)	370 (350)	0.68 (0.64)
3	510 (5.06)	543	1192	0.54	780	540	1.2
4	530 (8.65)	600	2201	0.11	800	990	1.4
5	508 (9.23)	558	1764	0.49	800	720	0.94
6	510 (10.8)	550	1326	0.55	800	760	0.88
7	507 (10.8)	547	1442	0.49	780	820	0.59
8	499 (12.2)	555	2022	0.46	780 (990)	840 (820)	0.57 (0.55)

^a λ_{max} of the one-photon absorption spectra in nm. ^b Molar extinction coefficient. ^c λ_{max} of the one-photon fluorescence spectra in nm. ^d Stokes shift in cm^{-1} . ^e Fluorescence quantum yield. ^f λ_{max} of the two-photon absorption spectra in nm. ^g The peak two-photon absorptivity at $\lambda_{\text{max}}^{(2)}$ in GM, 1 GM (Goppert-Mayer) = $1 \times 10^{-50} \text{ cm}^4 \text{ s photon}^{-1} \text{ molecule}^{-1}$. ^h The molecular weight was calculated by assuming that the donor is NMe_2 .

the phenyl group, it may facilitate the π -orbital delocalization and cause a large bathochromic shift. Moreover, λ_{max} of **1**, **2**, and **8** are nearly the same, indicating that it is relatively insensitive to the molecular size regardless of the conjugation length or the molecular symmetry. Except for **4**, the λ_{max} values of the quadrupoles (**3**–**7**) are also very similar. The largest λ_{max} for **4** could be because the butadiynyl group delocalizes the π -orbital more efficiently than the $\text{C}\equiv\text{C}$ bond. In sharp contrast, the λ_{max} of the double-bond analogue increases monotonically from 4-cyano-4'-diethylaminostilbene (398 nm) to 4-cyano-4'-(*p*-diethylaminostyryl)stilbene (416 nm) to 1,3,5-tricyano-2,4,6-tris(*p*-diethylaminostyryl)-benzene (481 nm).²⁶ The relative insensitivity of λ_{max} for **1**–**3** and **5**–**8** to the molecular size can be attributed

to the poorer conjugation ability of the $\text{C}\equiv\text{C}$ than the $\text{C}=\text{C}$ bond. Alternatively, this result could be explained in terms of the “effective conjugation length”. It was previously reported that the λ_{max} of poly(*p*-phenylene-ethynylene)s increased with the chain length and then converged to a limiting value.²⁷ The result has been attributed to the “effective conjugation length”, which describes the size of the π -system necessary to reach the size-independent optical and electronic properties of the macromolecules. Hence, the very similar λ_{max} observed for **1**–**3** and **5**–**8** seems to indicate that their π -system is close to “the effective conjugation length”. Finally, the molar absorptivity increases linearly with the conjugation length (Table 1). This is as expected because increasing the size of the π -orbital system will increase the density of states and so the probability of excitation.

The fluorescence spectra show Stokes shifts ranging from 1200 to 2250 cm^{-1} , indicating that the energy of the emitting states are significantly lower than the Franck–Condon singlet states. Except for **4**, the Stokes shifts for dipoles and octupole are slightly larger than the corresponding quadrupoles, probably because the excited-state charge transfer is more efficient in the former. Here again, the longest $\lambda_{\text{max}}^{\text{fl}}$ and a large Stokes shift are observed for **4**.

Most of the compounds are strongly fluorescent and the fluorescence quantum yields are close to 0.5. The much lower quantum yield for **4** may be due to the much lower energy of the emitting states, which may facilitate the nonradiative pathways (vide supra).

Two-Photon Cross Section Measured by the Fluorescence Measurement Method. The two-photon cross section δ_{TPA} was measured by the two-photon-induced fluorescence measurement technique using the nanosecond (ns) laser pulses by using the following equation,

$$\delta = \frac{S_s \Phi_r \phi_r c_r}{S_r \Phi_s \phi_s c_s} \delta_r \quad (1)$$

where the subscripts “s” and “r” stand for the sample and reference molecules.^{17b,21e} The intensity of the signal collected by a PMT detector was denoted as S . Φ is the fluorescence quantum yield. ϕ is the overall fluorescence collection efficiency of the experimental apparatus. The number density of the molecules in solution was denoted as c . δ_r is the TPA cross section of the reference molecule.

Figure 1 shows the normalized one-photon absorption, emission, and the two-photon excitation spectra for **4**. The corresponding spectra for other compounds are shown in Figure S1 in the Supporting Information. The results are summarized in Table 1.

Table 1 shows that **1**, **2**, and **8** exhibit two $\lambda_{\text{max}}^{(2)}$, one of which appears at 990 nm. This indicates that one of the two-photon allowed states for the dipoles and octupole are close to the one-photon allowed states, as predicted by symmetry.²⁸ Also, the two-photon allowed states for all of the quadrupoles are located at somewhat higher energy than the λ_{max} (Figure 1). This is again

(26) Lee, M. J.; Piao, M. J.; Lee, S. H.; Jeong, M.-J.; Kang, K. M.; Jeon, S.-J.; Cho, B. R. *J. Mater. Chem.* **2003**, *13*, 1030–1037.

(27) Francke, V.; Mangel, T.; Müllen, K. *Macromolecules* **1988**, *31*, 2447.

(28) McClain, W. M. *Acc. Chem. Res.* **1974**, *7*, 129.

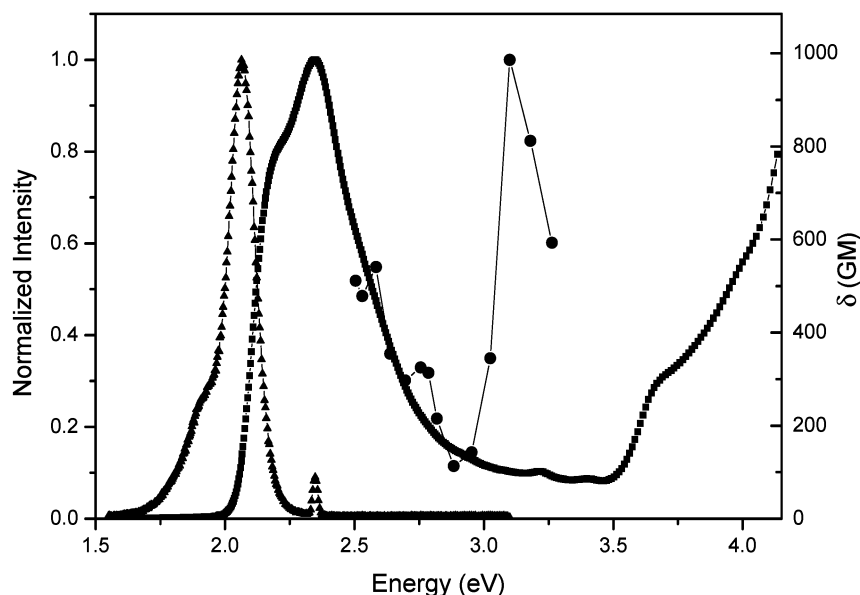


Figure 1. Normalized one-photon emission (▲), absorption (■) spectra, and two-photon excitation spectra (●) for **4** in toluene. The two-photon spectra are plotted as a function of total transition energy (twice the photon energy).

consistent with the prediction that the two-photon allowed states for quadrupoles should be at somewhat higher energy than the Franck–Condon states.²⁸ Moreover, all compounds show $\lambda_{\max}^{(2)}$ at 780–800 nm. This turns out to be very important for practical applications because most of the TPF microscopy uses a visible beam with a wavelength near 800 nm.

As can be seen in Table 1, the maximum value of the two-photon cross section ($\delta_{\max}^{\text{ns}}$) for **1–8** gradually increases with molecular size. The only exception to this trend is **4**, which shows the largest $\delta_{\max}^{\text{ns}}$. This is probably because λ_{\max} is the largest, that is, the smallest HOMO–LUMO energy gap, because the smaller the energy gap is, the higher the probability of the excitation will be. Finally, the value of $\delta_{\max}^{\text{ns}} = 990$ GM for **4** is comparable to $\delta_{\max}^{\text{ns}} = 1100$ GM reported for 2,6-bis(*p*-dihexylaminostyryl)anthracene.²⁴

To compare relative TPA properties per unit mass, we have calculated $\delta_{\max}^{\text{ns}}/\text{MW}$ of **1–8** (Table 1). Because the length of the alkyl chain in the NR₂ group is not expected to influence the TPA cross section, the donors are assumed to be NMe₂ in the calculation. The results show that $\delta_{\max}^{\text{ns}}/\text{MW}$ for the dipoles increases with the molecular size, indicating that the extension of the conjugation has some advantage. On the other hand, the $\delta_{\max}^{\text{ns}}/\text{MW}$ values of **3** and **5–7** slightly decrease with MW (Table 1). This could be because of the similar λ_{\max} values, that is, similar HOMO–LUMO gap, hence a smaller increase in the $\delta_{\max}^{\text{ns}}$ than the MW (vide supra). Interestingly, $\delta_{\max}^{\text{ns}}/\text{MW}$ is always larger for the quadrupoles than the dipoles, indicating that the former is superior to the latter as far as the $\delta_{\max}^{\text{ns}}/\text{MW}$ value is concerned. It was previously reported that the triphenylamine-based multibranched chromophores show significant enhancement of $\delta_{\max}^{\text{ns}}/\text{MW}$.^{19a,21e} Both electronic and vibronic couplings have been proposed for possible explanation. In contrast, the $\delta_{\max}^{\text{ns}}/\text{MW}$ value of **8** is smaller than **2**. The electronic coupling between the three branches of **8** does not appear possible because λ_{\max} and $\lambda_{\max}^{\text{fl}}$ of **2** and **8** are nearly the same. In

addition, the values of ϵ_{\max} for **2** and **8** are linearly proportional to the MW. This indicates that the density of states, hence the effective coupling channels between the ground and excited state, should be proportional to the MW. A combination of these two factors would predict that $\delta_{\max}^{\text{ns}}/\text{MW}$ of **8** should be smaller than **2**.

Two-Photon Cross Section Measured by Femtosecond Z-Scan Experiment. The femtosecond (fs) measurement is able to discriminate between the coherent two-photon processes and the excited-state absorption. The latter does not contribute to the measured signal when fs pulses are used because most of such processes occur on a picosecond (ps) or ns time scale.

To assess the contribution of the multiphoton absorption in the $\delta_{\max}^{\text{ns}}$ values, we have determined the TPA cross sections (δ_{fs}) of **2–8** by the open aperture Z-scan experiment using the fs pulses.^{29,30} It is well-established that the beam-intensity change along the propagation direction (*z* axis) can be described as

$$I(z) = \frac{I(0) \exp(-\alpha z)}{1 + \beta z I(0)} \quad (2)$$

where α is the attenuation coefficient that is due to linear absorption and scattering, β is the nonlinear absorption coefficient that is due to TPA, and *z* is the sample thickness, respectively. When the linear absorption is small, $\alpha z \ll 1$, the transmittance of the nonlinear medium can be written as

$$T(z) = I(z)/I(0) = \frac{\exp(-\alpha z)}{1 + \beta z I(0)} \approx \frac{1}{1 + \beta z I(0)}, \quad \alpha \approx 0 \quad (3)$$

where $I(0)$ is the input intensity I_0 .

(29) Tutt, L. W.; Boggess, T. F. *Prog. Quantum Electron.* **1993**, *17*, 299.

(30) He, G. S.; Yuan, L.; Cheng, N.; Bhawalkar, J. D.; Prasad, P. N.; Brott, L. L.; Clarkson, S. J.; Reinhardt, B. A. *J. Opt. Soc. Am. B* **1997**, *14*, 1079.

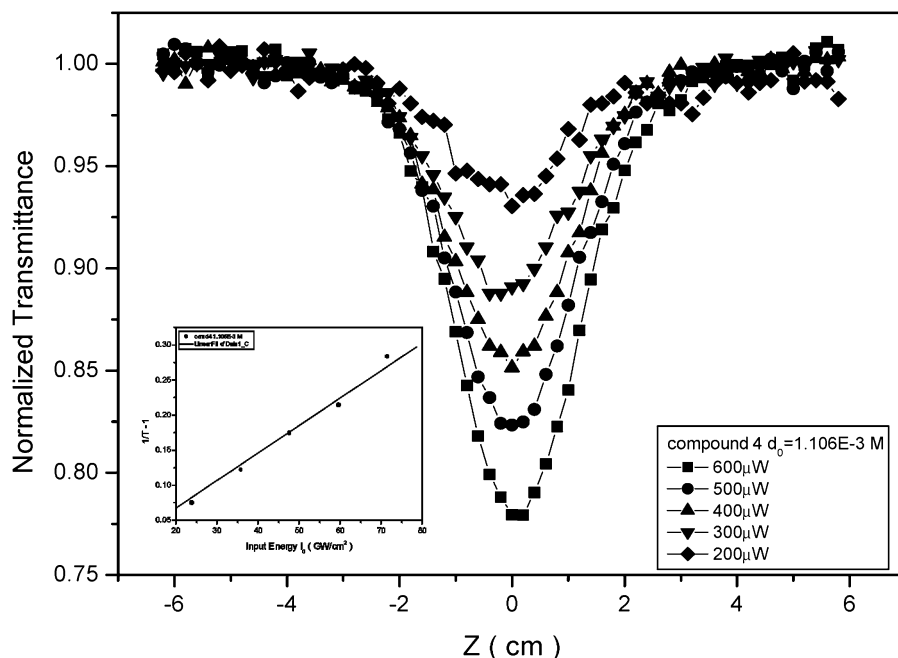


Figure 2. Z-Scan experimental data of compound **4** in toluene (1.11×10^{-3} M) in a 2.0-mm cell obtained by varying the input intensity of the laser beam. Inset: the plot of $([1/T(L)] - 1)$ vs I_0 (GW/cm²).

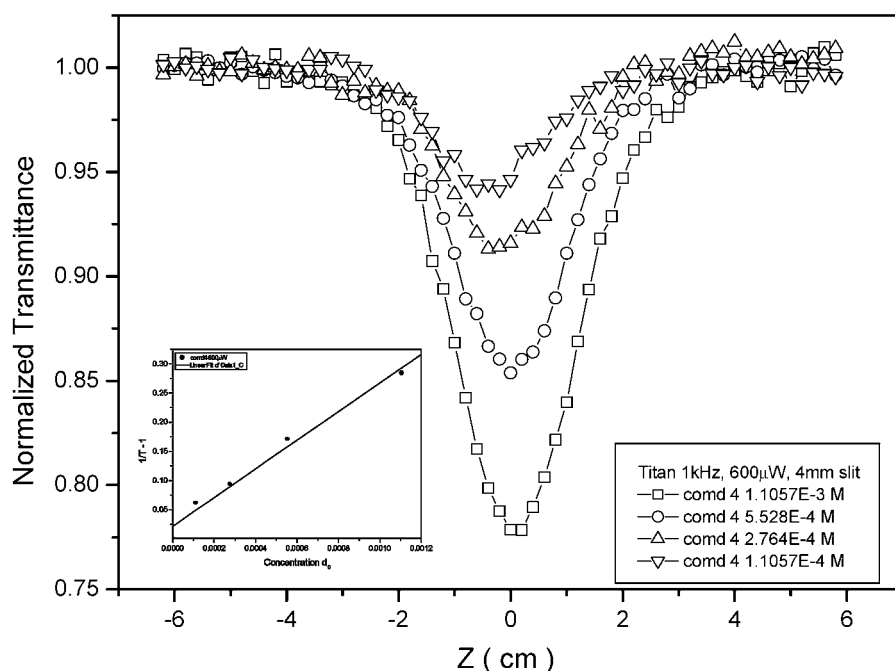


Figure 3. Z-Scan experimental data of compound **4** in toluene in a 2.0-mm cell obtained by varying the sample concentration. The input intensity of the laser beam was 600 μ W. Inset: the plot of $([1/T(L)] - 1)$ vs d_0 (M).

The relationship between β and the TPA cross section δ_2 (in units of cm⁴/GW) of the solute molecules can be expressed as

$$\beta = \delta_2 N_0 = \delta_2 N_A d_0 \times 10^{-3} \quad (4)$$

where N_A and d_0 are the Avogadro number and the mole concentration of the solute molecule, respectively. Substituting eq 4 into eq 3 and rearranging,

$$[1/T(L)] - 1 = \delta_2 N_A \times 10^{-3} L d_0 I_0 \quad (5)$$

where $T(L)$ is the transmittance at the sample thickness L of the nonlinear medium. Equation 5 indicates that

the TPA cross section δ_2 can be measured from the slopes of the plots of $([1/T(L)] - 1)$ against I_0 and d_0 .

Figure 2 shows the Z-scan data of **4** (1.11×10^{-3} M in toluene in a 2.0-mm cell), measured at 800 nm by changing the input intensity (I_0). The corresponding data obtained by varying the dye concentration (d_0) is shown in Figure 3. In both cases, the plots of $([1/T(L)] - 1)$ vs I_0 and d_0 are linear as predicted by eq 4. Moreover, the TPA cross sections (δ_{fs}) of **4–6** calculated from the slopes of both plots are very similar, indicating the reliability of the measurement (Table 2).

As expected, the values of δ_{fs} are always smaller than δ_{ns} , indicating a significant contribution by the excited

Table 2. Comparison of the TPA Cross Sections Measured by Femtosecond Z-Scan and Nanosecond Fluorescence Measurement Methods at 800 nm

cm ²	Z-scan (I_0) ^a			Z-scan (d_0) ^b			ns fl ^c	
	$10^{21} \delta_2^{d,e}$	$\delta_{fs}^{d,f}$	$\delta_{fs}/MW^{d,f}$	$10^{21} \delta_2^{d,e}$	$\delta_{fs}^{d,f}$	$\delta_{ns}^{d,f}$	$\delta_{ns}/MW^{d,f}$	
2	7.80	190	0.35			320	0.59	
3	8.30	210	0.45			490	1.1	
4	29.0	730	1.1	29.0	730	990	1.4	
5	18.0	460	0.60	19.0	470	720	0.94	
6	19.0	470	0.54	19.0	470	760	0.88	
7	17.0	420	0.44			680	0.70	
8	14.0	350	0.24			570	0.38	

^a Calculated from the slope of the plot of $([1/T(L)] - 1)$ vs I_0 for the femtosecond Z-scan experiment. ^b Calculated from the slope of the plot of $([1/T(L)] - 1)$ vs d_0 for the femtosecond Z-scan experiment. ^c Determined by the two-photon-induced fluorescence measurement technique using the nanosecond (ns) laser pulses. ^d Estimated uncertainty, $\pm 15\%$. ^e Unit is cm⁴/GW. ^f Unit is GM, 1 GM (Goppert-Mayer) = 1×10^{-50} cm⁴ s photon⁻¹ molecule⁻¹.

state absorption in the latter. However, the results of the structure-TPA property relationship studies from both experiments are qualitatively the same, that is, (i) TPA cross sections (δ_{fs}) are larger for the quadrupoles than the dipoles with comparable conjugation length, (ii) the δ_{fs}/MW of quadrupoles decrease with the conjugation length, (iii) the δ_{fs}/MW decreases by change from **2** to **8**, and (iv) **4** shows the largest δ_{fs} in this series of compounds. This could be explained if the contribution by the excited-state absorption is more or less the same for this series of compounds. Finally, $\delta_{fs} = 730$ GM determined for **4** is among the largest values determined by the Z-scan method.³¹

Most of the structure-TPA property relationship studies have been based on either ns fluorescence measurement or fs Z-scan experiments. Hence, it was difficult to make a direct comparison between them. The present result clearly shows that there is reasonable agreement between them. Therefore, although the magnitudes of δ_{TPA} are significantly different depending on the measurement methods, this result may provide a useful guideline for making such comparison.

Conclusions

In this work, we have synthesized a series of 9,10-bis(arylethynyl)anthracene derivatives (**1–8**) and measured their TPA cross sections by ns fluorescence measurement and fs Z-scan methods. The $\lambda_{max}^{(1)}$ values of these molecules are very similar and the $\lambda_{max}^{(2)}$ values are near 800 nm. The δ_{max}^{ns}/MW of the dipole increases with the chain length, whereas those for the quadrupoles decrease slightly with MW. Also, the δ_{max}^{ns}/MW of the octupole is smaller than the dipole. In all cases, the quadrupoles are found to be superior to the dipoles as far as the δ_{max}^{ns}/MW values are concerned. Moreover, the TPA cross sections measured by the femtosecond Z-scan experiment (δ_{fs}) are smaller than δ_{ns} , indicating a significant contribution by the excited-state absorption in the latter. Noteworthy is the qualitative agreement between the structure-TPA property relationships determined by both methods.

Experimental Section

Synthesis of 1–8. 9-Bromo-10-[p-(N,N-didecylamino)phenylethynyl]anthracene (**A**). A solution of 4-(N,N-didecylamino)phenylacetylene (4.2 g, 10 mmol) in toluene (10 mL) was added to a degassed solution of 9,10-dibromoanthracene (3.5 g, 10 mmol), Pd(PPh₃)₄ (0.24 g, 0.21 mmol), CuI (40 mg, 0.21 mmol), and (i-Pr)₂NH (30 mL) in toluene (90 mL) by a syringe. The suspension was stirred overnight at 80 °C. The solvent was removed in vacuo and the product was separated by column chromatography on silica gel using hexane as the eluent. Yield: 4.7 g (68%). mp: 80–82 °C. ¹H NMR (300 MHz, CDCl₃): δ 8.71 (d, $J = 9.0$ Hz, 2H), 8.54 (d, $J = 9.0$ Hz, 2H), 7.60 (m, 6H), 6.70 (d, $J = 9.0$ Hz, 2H), 3.32 (t, $J = 7.5$ Hz, 4H), 1.62 (m, 4H), 1.31 (m, 28H), 0.89 (t, $J = 7.5$ Hz, 6H).

9-(p-Cyanophenylethynyl)-10-[p-(N,N-didecylamino)phenylethynyl]anthracene (**1**). **1** was synthesized from **A** and p-cyanophenylacetylene by the same procedure as described for **A** except that Pd(PPh₃)₂Cl₂, Et₃N, and THF were used in place of Pd(PPh₃)₄, (i-Pr)₂NH, and toluene and the reaction temperature was 60 °C. The product was purified by column chromatography on silica gel using MC/hexane (2/1) as the eluent. Yield: 32%. mp: 123–125 °C. IR (KBr, cm⁻¹): 2225 (C≡N), 2176 (C≡C). ¹H NMR (300 MHz, CDCl₃): δ 8.74 (d, $J = 9.0$ Hz, 2H), 8.60 (d, $J = 9.0$ Hz, 2H), 7.84 (d, $J = 9.0$ Hz, 2H), 7.74 (d, $J = 9.0$ Hz, 2H), 7.63 (m, 6H), 6.67 (d, $J = 9.0$ Hz, 2H), 3.32 (t, $J = 7.5$ Hz, 4H), 1.62 (m, 4H), 1.31 (m, 28H), 0.89 (t, $J = 7.5$ Hz, 6H). ¹³C NMR (75 MHz, CDCl₃): δ 148.65, 133.39, 132.67, 132.41, 132.18, 131.73, 128.71, 128.00, 127.38, 126.92, 126.61, 121.67, 118.86, 115.50, 111.66, 111.56, 108.71, 105.98, 100.15, 91.64, 84.91, 51.26, 32.14, 29.90, 29.82, 29.77, 29.57, 27.47, 27.38, 22.93, 14.37. Anal. Calcd for C₅₁H₅₈N₂: C, 87.63; H, 8.36; N, 4.01. Found: C, 87.74; H, 8.29; N, 4.08.

9-[4-(p-Cyanophenylethynyl)phenylethynyl]-10-[p-(N,N-didecylamino)phenylethynyl]anthracene (**2**). **2** was synthesized from **A** and 4-(p-cyanophenylethynyl)phenylacetylene by the same procedure as described for **1**. Yield: 36%. mp: 140–142 °C. IR (KBr, cm⁻¹): 2225 (C≡N), 2176 (C≡C). ¹H NMR (300 MHz, CDCl₃): δ 8.72 (d, $J = 9.0$ Hz, 2H), 8.64 (d, $J = 9.0$ Hz, 2H), 7.76 (d, $J = 9.0$ Hz, 2H), 7.63 (m, 12H), 6.68 (d, $J = 9.0$ Hz, 2H), 3.32 (t, $J = 7.5$ Hz, 4H), 1.63 (m, 4H), 1.31 (m, 28H), 0.90 (t, $J = 6.0$ Hz, 6H). ¹³C NMR (75 MHz, CDCl₃): δ 148.59, 132.53, 132.30, 132.28, 132.11, 131.83, 131.81, 128.72, 128.21, 127.91, 127.17, 127.11, 126.56, 124.61, 122.26, 120.90, 118.73, 116.48, 111.85, 111.58, 108.89, 105.53, 101.56, 93.78, 89.87, 89.67, 84.96, 51.26, 32.15, 29.91, 29.83, 29.78, 29.58, 27.48, 27.39, 22.94, 14.38. Anal. Calcd for C₅₉H₆₂N₂: C, 88.67; H, 7.82; N, 3.51. Found: C, 88.82; H, 7.78; N, 3.46.

9,10-Bis[p-(N,N-didecylamino)phenylethynyl]anthracene (**3**). **3** was synthesized from **A** and p-(N,N-didecylamino)phenylacetylene by the same procedure as described for **A**. Yield: 75%. mp: 61–63 °C. IR (KBr, cm⁻¹): 2176 (C≡C). ¹H NMR (300 MHz, CDCl₃): δ 8.69 (d, $J = 9.0$ Hz, 4H), 7.59 (m, 8H), 6.66 (d, $J = 9.0$ Hz, 4H), 3.32 (t, $J = 7.5$ Hz, 8H), 1.62 (m, 8H), 1.32 (m, 56H), 0.90 (t, $J = 7.5$ Hz, 12H). ¹³C NMR (75 MHz, CDCl₃): δ 148.18, 133.00, 131.81, 127.45, 126.20, 118.50, 111.35, 109.04, 104.04, 84.78, 51.03, 31.91, 29.66, 29.58, 29.54, 29.33, 27.24, 27.16, 22.69, 14.12. Anal. Calcd for C₇₀H₁₀₀N₂: C, 86.71; H, 10.40; N, 2.89. Found: C, 86.75; H, 10.50; N, 2.86.

9-[p-(N,N-Didecylamino)phenylethynyl]-10-ethynylanthracene (**B**). Trimethylsilylacetylene (1.5 mL, 11 mmol) was slowly added with a syringe to a degassed solution of **A** (4.0 g, 6.1 mmol), Pd(PPh₃)₂Cl₂ (0.39 g, 0.55 mmol), CuI (0.11 g, 0.55 mmol), and Et₃N (10 mL) in THF (20 mL) in an ice bath. After 30 min, the ice bath was removed and the suspension was stirred for 6 h at RT. The solvent was evaporated and the residue was separated by column chromatography on silica gel using hexane as the eluent. The major product was added to methanol/THF (2/1, 150 mL) and then aqueous KOH (10%, 20 mL). After the solution was stirred for 30 min, the mixture was poured into water and extracted with ether. The solvent was evaporated and the product was separated by column chromatography on silica gel using hexane as the eluent. Yield: 3.2 g (87%). ¹H NMR (300 MHz, CDCl₃): δ 8.70 (m, 2H), 8.60 (m, 2H), 7.60 (m, 6H), 7.66 (d, $J = 9.0$ Hz, 2H), 4.05

(31) The most efficient TPA chromophores showing the largest TPA cross sections measured by fs Z-scan experiments are TP-DTT-TP (270 GM)¹⁶ and PRL-701 (600 GM).^{19a}

(s, 1H), 3.32 (t, $J = 7.5$ Hz, 4H), 1.61 (m, 4H), 1.29 (m, 28H), 0.89 (t, $J = 6.0$ Hz, 6H).

9-[*p*-(*N,N*-Didecylamino)phenylethynyl]-10-(*p*-iodophenylethynyl)anthracene (C'**).** **C'** was prepared from **B** (3.1 g, 5.18 mmol), 1,4-diiodobenzene (1.82 g, 5.52 mmol), Pd(PPh₃)₂Cl₂ (0.116 g, 0.165 mmol), CuI (31.5 mg, 0.165 mmol), and Et₃N (10 mL) in THF (25 mL) by the same procedure as described for **1** except that the temperature was 50 °C. The product was purified by column chromatography on silica gel using MC/hexane (first 1/50, then 1/25, and finally 1/10) as the eluent. Yield: 2.8 g (68%). mp: 100–102 °C. ¹H NMR (300 MHz, CDCl₃): δ 8.72 (m, 2H), 8.62 (m, 2H), 7.79 (d, $J = 6.0$ Hz, 2H), 7.62 (m, 6H), 7.49 (d, $J = 6.0$ Hz, 2H), 6.68 (d, $J = 9.0$ Hz, 2H), 3.33 (t, $J = 7.5$ Hz, 4H), 1.62 (m, 4H), 1.29 (m, 28H), 0.89 (t, $J = 7.5$ Hz, 6H).

9-[4-(*N,N*-Didecylamino)phenylethynyl]-10-(4-ethynylphenylethynyl)anthracene (C**).** **C** was synthesized from **C'** and trimethylsilylacetylene by the same procedure as described for **B**. The product was purified by column chromatography on silica gel using hexane/MC (20/1) as the eluent. Yield: 91%. mp: 79–80 °C. ¹H NMR (300 MHz, CDCl₃): δ 8.73 (m, 2H), 8.65 (m, 2H), 7.74 (d, $J = 9.0$ Hz, 2H), 7.62 (m, 6H), 7.58 (d, $J = 9.0$ Hz, 2H), 6.68 (d, $J = 9.0$ Hz, 2H), 3.34 (t, $J = 7.5$ Hz, 4H), 3.23 (s, 1H), 1.63 (m, 4H), 1.31 (m, 28H), 0.91 (t, $J = 7.5$ Hz, 6H).

1,4-Bis[10-[4-(*N,N*-didecylamino)phenylethynyl]anthracen-9-yl]-1,3-butadiyne (4**).** **4** was synthesized by the homo coupling of **B** by the same procedure as described for **1**. Yield: 69%. mp: 177–179 °C. IR (KBr, cm⁻¹): 2176 (C≡C). ¹H NMR (300 MHz, CDCl₃): δ 8.74 (d, $J = 9.0$ Hz, 4H), 8.71 (d, $J = 9.0$ Hz, 4H), 7.70 (m, 4H), 7.65 (m, 4H), 7.62 (d, $J = 9.0$ Hz, 4H), 6.68 (d, $J = 9.0$ Hz, 4H), 3.33 (t, $J = 7.5$ Hz, 8H), 1.63 (m, 8H), 1.32 (m, 56H), 0.90 (t, $J = 7.5$ Hz, 12H). ¹³C NMR (75 MHz, CDCl₃): δ 152.28, 148.44, 133.25, 132.15, 130.90, 130.17, 128.27, 126.84, 126.01, 124.36, 120.90, 119.50, 111.53, 108.98, 103.92, 84.51, 51.26, 32.14, 29.91, 29.83, 29.78, 29.57, 27.47, 27.39, 22.94, 14.38. Anal. Calcd for C₈₈H₁₀₈N₂: C, 88.53; H, 9.12; N, 2.35. Found: C, 88.24; H, 9.18; N, 2.42.

1,4-Bis[10-[4-(*N,N*-didecylamino)phenylethynyl]anthracen-9-ylethynyl]benzene (5**).** **5** was synthesized from **A** and **C** by the same procedure as described for **1**. Yield: 57%. mp: 222–224 °C. IR (KBr, cm⁻¹): 2176 (C≡C). ¹H NMR (300 MHz, CDCl₃): δ 8.72 (m, 8H), 7.85 (s, 4H), 7.65 (m, 12H), 6.68 (d, $J = 9.0$ Hz, 4H), 3.34 (t, $J = 7.5$ Hz, 8H), 1.63 (m, 8H), 1.31 (m, 56H), 0.90 (t, $J = 7.5$ Hz, 12H). ¹³C NMR (75 MHz, CDCl₃): δ 148.56, 133.34, 132.52, 131.90, 131.88, 127.88, 127.29, 127.08, 126.57, 123.81, 120.67, 116.77, 111.57, 108.97, 105.33, 101.99, 89.35, 84.98, 51.26, 32.15, 29.91, 29.83, 29.78, 29.58, 27.48, 27.39, 22.94, 14.38. Anal. Calcd for C₉₄H₁₁₂N₂: C, 88.90; H, 8.89; N, 2.21. Found: C, 88.74; H, 9.01; N, 2.28.

4,4'-Bis[10-[4-(*N,N*-didecylamino)phenylethynyl]anthracen-9-ylethynyl]diphenylethyne (6**).** **6** was synthesized from **C** and **C'** by the same procedure as described for **1**. Yield: 63%. mp: 182–184 °C. IR (KBr, cm⁻¹): 22176 (C≡C). ¹H NMR (300 MHz, CDCl₃): δ 8.70 (m, 8H), 7.76 (d, $J = 9.0$ Hz, 4H), 7.64 (m, 16H), 6.68 (d, $J = 9.0$ Hz, 4H), 3.33 (t, $J = 6.0$ Hz, 8H), 1.64 (m, 8H), 1.34 (m, 56H), 0.93 (t, $J = 7.5$ Hz, 12H). ¹³C NMR (75 MHz, CDCl₃): δ 148.56, 133.36, 132.83, 132.52, 131.99, 131.87, 131.79, 127.91, 127.08, 126.56, 123.89, 123.25, 120.71, 116.75, 111.59, 108.99, 105.38, 101.89, 91.63, 89.31, 85.03, 51.28, 32.18, 29.95, 29.87, 29.81, 29.62, 27.51, 27.42, 22.97, 14.41. Anal. Calcd for C₁₀₂H₁₁₆N₂: C, 89.42; H, 8.53; N, 2.04. Found: C, 89.24; H, 8.62; N, 2.08.

1,4-Bis-[4-[10-[4-(*N,N*-didecylamino)phenylethynyl]anthracen-9-ylethynyl]phenylethynyl]benzene (7**).** **7** was synthesized by the same procedure as described for **1** except that **C** and *p*-diiodobenzene were used in a 2:1 ratio. Yield: 71%. mp: 197–199 °C. IR (KBr, cm⁻¹): 2176 (C≡C). ¹H NMR (300 MHz, CDCl₃): δ 8.69 (m, 4H), 8.62 (m, 4H), 7.70 (d, $J = 9.0$ Hz, 4H), 7.60 (m, 16H), 7.52 (d, $J = 9.0$ Hz, 4H), 6.64 (d, $J = 9.0$ Hz, 4H), 3.28 (t, $J = 7.5$ Hz, 8H), 1.60 (m, 8H), 1.29 (m, 56H), 0.89 (t, $J = 7.5$ Hz, 12H). ¹³C NMR (75 MHz, CDCl₃): δ 148.56,

133.34, 132.51, 131.97, 131.86, 131.79, 127.90, 127.26, 127.08, 126.56, 123.91, 123.32, 123.20, 120.70, 116.69, 111.57, 108.93, 106.90, 105.35, 101.79, 91.52, 91.43, 89.26, 84.95, 51.26, 32.15, 29.91, 29.83, 29.78, 29.57, 27.48, 27.39, 22.94, 14.38. Anal. Calcd for C₁₁₀H₁₂₀N₂: C, 89.87; H, 8.23; N, 1.91. Found: C, 89.74; H, 8.29; N, 1.94.

1,3,5-Tricyano-2,4,6-tris[4-[10-[4-(*N,N*-didecylamino)phenylethynyl]anthracen-9-ylethynyl]-phenylethynyl]benzene (8**).** A mixture of 1,3,5-tricyano-2,4,6-tribromobenzene (39 mg, 0.10 mmol), **C** (0.34 g, 0.49 mmol), Pd(PPh₃)₄ (12 mg, 0.010 mmol), and CuI (2.0 mg, 0.010 mmol), Et₃N (2.0 mL), and toluene (1.0 mL) was heated to 85 °C for 16 h. The solvent was evaporated and the residue was separated by column chromatography on silica gel using MC/hexane (1/1) as the eluent. Yield: 67 mg (30%). mp: 126–128 °C. IR (KBr, cm⁻¹): 2225 (C≡N), 2176 (C≡C). ¹H NMR (300 MHz, CDCl₃): δ 8.74 (m, 6H), 8.66 (m, 6H), 7.76 (d, $J = 9.0$ Hz, 6H), 7.64 (m, 24H), 6.68 (d, $J = 9.0$ Hz, 6H), 3.34 (t, $J = 9.0$ Hz, 12H), 1.64 (m, 12H), 1.31 (m, 84H), 0.91 (t, $J = 7.5$ Hz, 18H). ¹³C NMR (75 MHz, CDCl₃): δ 148.66, 133.40, 132.83, 132.67, 132.52, 132.41, 132.18, 131.82, 131.79, 131.74, 128.71, 128.00, 127.37, 126.92, 126.61, 121.68, 118.86, 115.51, 111.66, 111.57, 108.73, 105.98, 100.15, 91.65, 84.92, 51.26, 32.14, 29.90, 29.82, 29.77, 29.57, 27.48, 27.38, 22.93, 14.37. Anal. Calcd for C₁₆₅H₁₇₄N₆: C, 88.42; H, 7.83; N, 3.75. Found: C, 88.24; H, 7.89; N, 3.82.

Measurement of Two-Photon Cross Section by the Two-Photon-Induced Fluorescence Method. The two-photon absorption cross section of the octupolar compounds has been measured with the two-photon-induced fluorescence method by using the nanosecond laser pulses as described.^{17b,21e} Samples were dissolved in toluene at concentrations of 1.0×10^{-5} M and the two-photon-induced fluorescence intensity was measured at 750–1050 nm by using rhodamine B (1×10^{-5} M in MeOH) as the reference.⁴ The intensities of the two-photon-induced fluorescence spectra of the reference and sample emitted at the same excitation wavelength were determined. The TPA cross section at each wavelength was calculated according to eq 1.

Measurement of Two-Photon Cross Section by the Femtosecond Z-Scan Method. The open aperture z-scan experiment has been conducted by using essentially the same experimental setup and procedure as described.^{29,30} A linearly polarized 800-nm fs pulsed laser beam was used as the source. A mode-locked Titanium:Sapphire laser (Mira900-F, Coherent) produced a single Gaussian 180-fs pulse (800 nm). The pulse was amplified by a Nd:YLF laser (Titan, Quantronix, pulse width ≈ 200 fs (fwhm), repetition rate = 1 kHz) so that the laser power would be approximately 0.9–1 W at the wavelength of 800 nm and reduced to several by using a variable neutral density filter. After passing through an $f = 30.5$ cm lens, this laser beam was focused ($\omega_0 = 3.88 \times 10^{-3}$ cm) and passed through a 2.0-mm glass cell filled with the sample solution [$(1.01\text{--}1.24) \times 10^{-3}$ M in toluene]. The transmitted laser beam from the sample cell was detected, while changing position of the sample cell along the beam direction (z -axis), by using a photodiode. Input intensity ranged from 200 to 600, which corresponds to the peak irradiance I_0 ranging from 23.8 to 71.5 GW/cm² at the focus, respectively. The TPA cross sections were calculated from slopes of the plots of $([1/T(L)] - 1)$ against I_0 and d_0 by using eq 5.

Acknowledgment. This work is supported by the NRL-MOST and CRM-KOSEF. W. J. Yang, M. J. Piao, and S. K. Lee were supported by the BK21 program.

Supporting Information Available: Additional figures (PDF). This material is available free of charge via the Internet at <http://pubs.acs.org>.

CM035032A